Title
Analysis of Crustal Heterogeneity with Application to Wave Propagation at the KTB Site

Authors
Gritto, R.
Kaelin, B.
Johnson, L.R.

Publication Date
1995-05-01

LBL-37237
UC-403
Preprint

Lawrence Berkeley Laboratory
UNIVERSITY OF CALIFORNIA

EARTH SCIENCES DIVISION

Submitted to Geophysics

Analysis of Crustal Heterogeneity with Application to Wave Propagation at the KTB Site

R. Gritto, B. Kaelin, and L.R. Johnson

May 1995

Prepared for the U.S. Department of Energy under Contract Number DE-AC03-76SF00098

DISCLAIMER

LBL - 37237
UC - 403

Analysis of Crustal Heterogeneity with Application to Wave Propagation at the KTB Site

Roland Gritto, Bruno Kaelin and Lane R. Johnson

Earth Sciences Division
Lawrence Berkeley Laboratory
University of California
Berkeley, CA 94720

Data processing was done at the Center for Computational Seismology, Lawrence Berkeley Laboratory, under support from the Director, Office of Energy Research, Office of Basic Energy Sciences, Geosciences Program, through U.S. Department of Energy under contract DE-AC03-76SF00098.

Analysis of Crustal Heterogeneity with Applications to Wave Propagation at the KTB Site

Roland Gritto, Bruno Kaelin and Lane R. Johnson

Department of Geology and Geophysics, University of California at Berkeley, and Center for Computational Seismology, Earth Science Division, Lawrence Berkeley Laboratory, Berkeley, California 94720

ABSTRACT

Borehole logs from the German Continental Deep Drilling Project (KTB) are analyzed to study the small scale structure of the upper crust. An exponential function is found to best fit the autocorrelation function of the high frequency log data, with a correlation length of about 2 m. We separate the low frequency trend in the P wave velocity log, representing distinct geological lithology, emplaced by either original deposition processes or later tectonic activity, and investigate its power spectrum to determine a possible power law. A constant slope of approximately -2, indicating fractal dimensions over a scale length ranging from 3.5 km to 100 m, best fits the spectrum. The power spectrum of the high frequency residual of the log revealed stationarity in the small scale structure over a depth range of 6 km. The difference of the modal characteristics of the medium, represented by either velocity or the elastic moduli and the density are presented. The bimodal character of the crust at the KTB site is only poorly resolved by the velocity distribution, whereas the elastic moduli and the density show a clear distinction of the two geological units. The properties of the KTB logs are used to model elastic wave propagation in a homogeneous horizontally layered medium as a means of investigating scattering attenuation and wave localization. The results indicate that localization, or exponential attenuation of the elastic waves, is evident for frequencies above 200 Hz for a travel distance $L \geq 2.5$ km. If the travel distance increases to $L \geq 10$ km, localization occurs for all frequencies above 30 Hz. The localization analysis independently confirms the result of an exponential func-

tion as the best fit to the autocorrelation function of the small scale structure.

1. Introduction

The KTB project offers a unique opportunity to study the material properties of the upper crust. Detailed information about the geophysical, geological and mineralogical parameters have become increasingly important with the development of advanced seismic source and receiver systems in recent years. Sources capable of transmitting energy above 1 kHz require a better model of small scale crustal structures to understand the processes of wave propagation and the interpretation of high resolution data.

In recent years, numerical studies on the small scale structure of inhomogeneous media have used statistical approaches for the description of the physical properties (Wu and Aki, 1985; Frankel and Clayton, 1986). These approaches are based on basic assumptions like stationarity of the medium in both depth and lateral extent, or ergodicity of the medium (spatial averaging over one realization can be substituted for ensemble averaging over several medium realizations (Shapiro and Zien, 1993)). In order to compare analytical investigations with real field recordings, the assumption of ergodicity is essential, since the true world offers only one realization of the medium. However, it is not always clear whether the medium under investigation is stationary or ergodic with respect to the parameters of interest.

Although the two boreholes with a separation of ~ 180 m provide only limited lateral information, the main borehole with a target depth of 10 km permits the study of physical parameters as a function of depth in the upper crust. The variation in parameters depends upon the scale length under investigation. Petrogenic processes like sedimentation, volcanic deposition, or metamorphosis generate characteristic features on scale lengths which differ from those generated by tectonic activities. We investigate borehole logs to determine the scale lengths associated with the underlying geological processes. The power spectrum of the low frequency information in V_p logs is investigated to determine a possible power law for large scale lengths. However, at scale lengths where the power law breaks down, further analysis of high frequency information of the velocity log is performed to study the small scale characteristic length and the correlation function of the medium.

Modal characteristics are essential for the treatment of heterogeneous media, when wave propagation can no longer be modeled by methods applying discrete descriptions of the medium, but rather having to rely on statistical approaches to represent the elastic properties. The modal character of a medium generally is analyzed by investigating the underlying velocity distribution. However, the real characteristic parameters of the medium are density, bulk and shear modulus. Considering the equations for P wave and S wave velocity, $\sqrt{\frac{K + \frac{4}{3}\mu}{\rho}}$ and $\sqrt{\frac{\mu}{\rho}}$, respectively, it is easy to see that the characteristics of a medium, apparent in the moduli and density, may be canceled in these equations and thus concealed in the velocities. We will present the difference between the distributions of the moduli and the velocities from the borehole logs and discuss implications for the analysis.

The concept of stratigraphic filtering was introduced to seismology by O'Doherty and Anstey (1971) to investigate scattering processes during the propagation of elastic waves. The authors suggested multiple reflections of elastic waves within thin layers as a cause for near total attenuation of energy in certain frequency bands. It is now recognized that this phenomenon is similar to wave localization, well established in quantum mechanics, solid state physics and optics. Localization does not require the presence of anelastic attenuation in the medium, and, as we show, could be the main attenuation mechanism for a hypothetical layered medium with the elastic properties of the KTB site, especially in high frequency seismic surveys. Since then, various authors have studied the consequences of the proposed theory in numerical simulations using well log data (Banik et al., 1985a, 1985b; Sheng, 1990; White et al., 1990), although these studies were either limited in spectral range or in depth extent of the well log data. However, detailed investigations of propagating broadband wavefields over various depth ranges is essential for the understanding of the scattering process.

The KTB well logs provide an excellent opportunity to investigate localization effects in the upper crust. We study the effects of the small scale inhomogeneities on the propagation of elastic waves through the crustal structure by simulating one dimensional elastic wave propagation based on the velocity and density log data from the main borehole, and present the effects of scattering attenuation by the medium. Finally, we create numerical well logs using mean values and standard deviations of the

natural log data and superimpose specific correlation functions. These logs are used to propagate waves through the numerical model and compare the results to those computed using the natural log data. Thus we are able to independently estimate correlation functions in the medium and compare them to the results of the correlation analysis.

2. Statistical properties of the upper crust

Small Scale Structure

The velocity, density and gamma ray logs for the KTB main hole are shown in Figure 1. While velocity measurements range from 0.25 km to 6 km depth, the density was only measured below 3 km. Apparent in the logs is the high frequency information manifested in the noisy signal. It carries information about the small scale properties of the medium and is the subject of our correlation analysis. The broad trend in the logs is best visible in the gamma ray log representing the stratigraphy consisting of gneiss and metabasite in alternating order (Lich et al., 1992). This signal will be investigated to determine a possible power law dependence. The clear and abrupt changes in the gamma ray log are used to subdivide all logs into depth ranges of uniform stratigraphy, hence separating high frequency from low frequency information.

Localization of elastic waves is caused by small scale inhomogeneities, and thus it is essential to investigate this structure as a function of depth on a scale smaller than geologic units. Hence, the KTB log measurements at a depth interval of ~ 0.15 m represent a good data set to study the upper crust. The properties under investigation are the characteristic length of the medium on the smallest possible scale, in accordance with the sampling rate of the log measurements, and the correlation function of these inhomogeneities as functions of depth.

In order to extract the high frequency information from the data, a stacking procedure was utilized. First, the logs were divided into nine large intervals based on the lithological changes apparent in the gamma ray log as described above. Each of these intervals was subdivided into a number of sections, observing the limits for the autocorrelation process (the intervals were 10 times longer than the maximum lag of 10 m) with a 50% overlap in length. The autocorrelation was computed for each of the

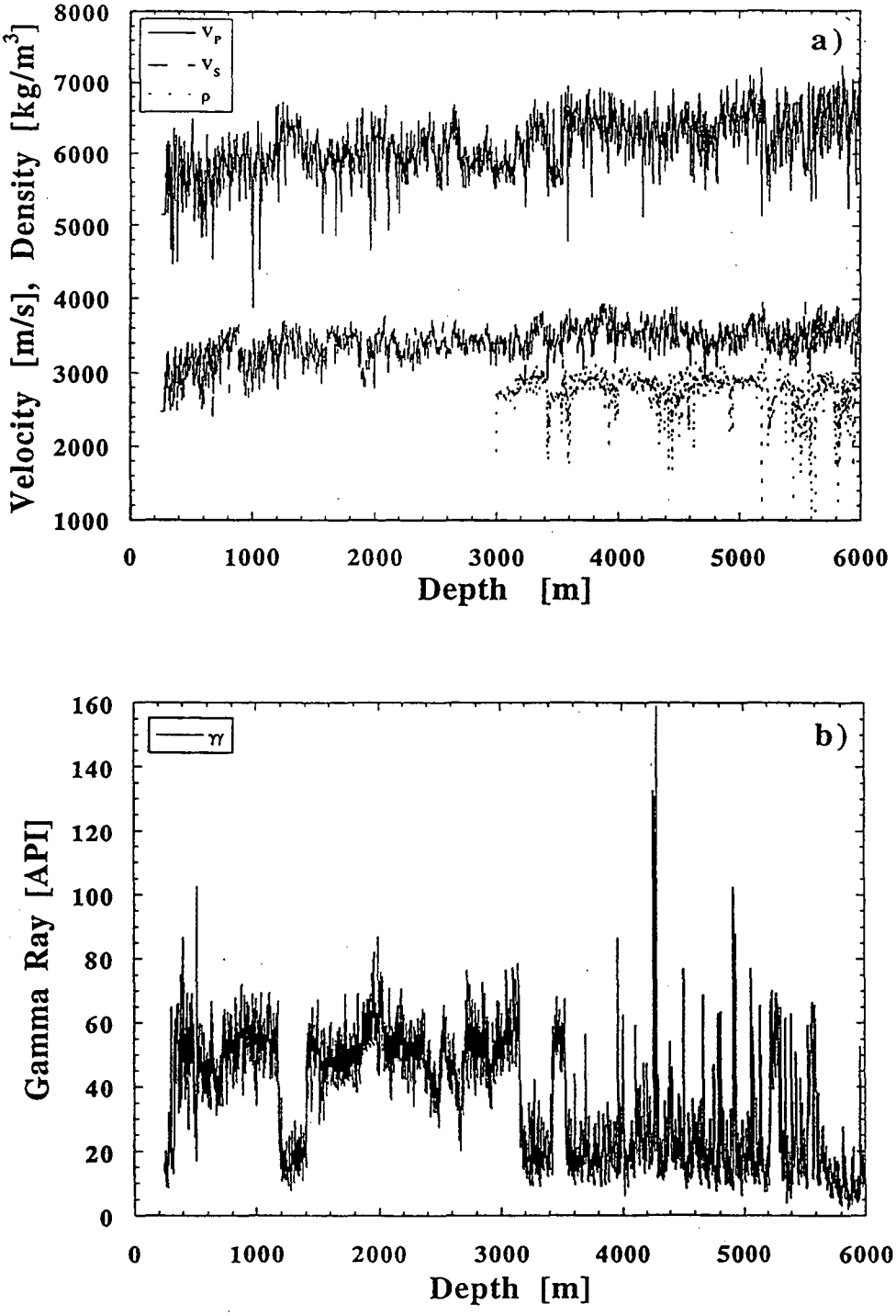

Figure 1 Borehole logs for the KTB main hole:

a) Velocities and density (solid line: P wave velocity, dashed line: S wave velocity, dotted line: density, measured below 3 km only),

b) Gamma ray log.

sections within a given interval and the results stacked. This stacking technique removed any remaining low frequency trend within one geological unit, while the high frequency information remains in the data. This procedure was repeated for every large interval, representing a geological unit, thus producing autocorrelation functions as functions of depth. The variance of the autocorrelation functions is computed after Marple et al. (1987) as follows

$$var\ [\hat{r}_{xx}(m)] \approx \frac{1}{N} \sum_{k=-\infty}^{\infty} [r_{xx}^2(k) + r_{xx}(k+m)r_{xx}(k-m)] \quad , \tag{1}$$

where $\hat{r}_{xx}(m)$ is the biased estimate for the autocorrelation $r_{xx}(k)$.

The results of the correlation analysis are shown in Figure 2. We plot the autocorrelation and the standard deviation of the logs as a function of lag. For reasons of brevity, we only present the results of four depth intervals, representative of the whole depth range. Figure 2a - 2c reveal the results for the P and S wave velocity and the density analysis, respectively. The autocorrelation functions show a similar trend for the other depth intervals. Longer depth intervals produced smoother correlation functions as more sections were stacked. An approximate exponential decay for short lags is followed by a more gradual decay at longer lags. The exponential trend at short lags is representative of small scale structure of the medium and is the aim of our investigation. The trend for longer lags may represent larger scale structure, e.g. geological sequences. However, because of our stacking procedure designed to enhance small scale heterogeneities, the information of the large scale structure may not carry reliable information. Additionally, the standard deviation (dashed line) indicates that the reliable range of the autocorrelation function lies within short lags, where the estimates are large compared to the error. Therefore, autocorrelation values for lags longer than 5 m should be viewed with caution.

All three logs produce the same general result with respect to the spatial correlation of material properties. Three functions, a Gaussian, an exponential, and a Von Karman function are applied to the correlation curves to determine the best fit. An exponential decay is found to best fit the data with an average correlation length of 2 m, with standard error of 1.5 m. Small variations of these values occur throughout the whole depth interval with magnitudes smaller than one standard deviation. Our investigations revealed the same results for the pilot hole, 180 m away from the main hole, indicating no

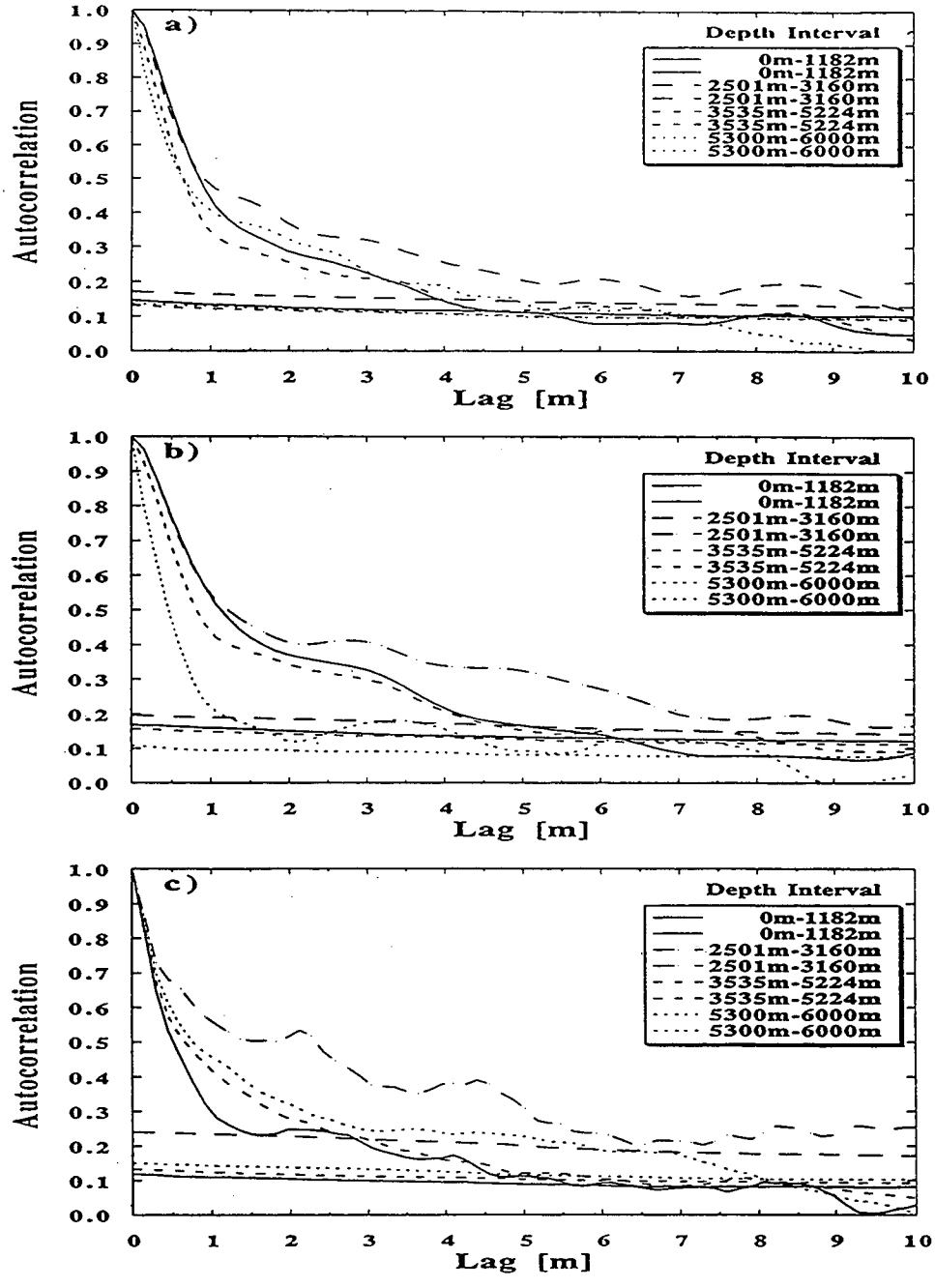

Figure 2 Autocorrelation functions and standard deviations for various depth intervals of the KTB main hole:

a) P wave velocity autocorrelation and standard deviation,

b) S wave velocity autocorrelation and standard deviation,

c) density autocorrelation and standard deviation.

lateral change over this distance.

Large Scale Structure

To determine a possible power law for the large scale information in the logs, we compute the mean value for the logs for every depth interval. Thus we create logs with a sequence of constant values for the corresponding stratigraphy shown in Figure 3a. The existence of a possible power law of the form $P - f^n$ can be investigated by computing the power spectrum and displaying it on a log-log scale. A constant slope over a certain wavenumber range would determine the underlying power law. Figure 3b shows the power spectrum of the V_p log. The best least squares fit for the logarithmic wavenumber range between $-3.25\ m^{-1}$ and $-0.25\ m^{-1}$ reveals a slope of -1.997 ± 0.019. This result clearly portraits the power law difference between the large and the small scale structure. The constant slope of about -2 is caused by the dominance of the rectangular functions in Figure 3a. Since the power spectrum of a rectangular function is the square of a sinc function, the square in the denominator dominates the slope on a log-log scale. Therefore, whenever the large scale features in a log can be approximated by a series of rectangular functions, the associated power law will reveal a slope of approximately -2.

Subtracting the log of mean values (Fig. 3a) from the P-wave log (Fig. 1a) enables us to independently confirm the results of the small scale correlation analysis. Figure 4b shows the remaining high frequency information in the V_p log after subtracting the mean values of Figure 3a. To investigate whether the small scale structure has uniform statistical properties over the entire 6 km depth, we compute the power spectrum of each depth interval, and stack the result to get a more stable estimate. Intervals with different depth ranges are padded to reach equal length before the power spectrum is computed. The nine spectra subsequently are weighted, stacked and the standard deviation computed to estimate the reliability of the power spectrum over the entire depth range. The result is shown in Figure 4b. The solid line, representing the power spectrum, reveals a reduction in the variance of the estimate which is due to the stacking procedure. Additionally, the amplitudes remain larger than the standard deviation throughout the entire depth range, indicating a stabilization of the power spectrum by the stacking process. This result indicates that, first, the governing process responsible for the small scale

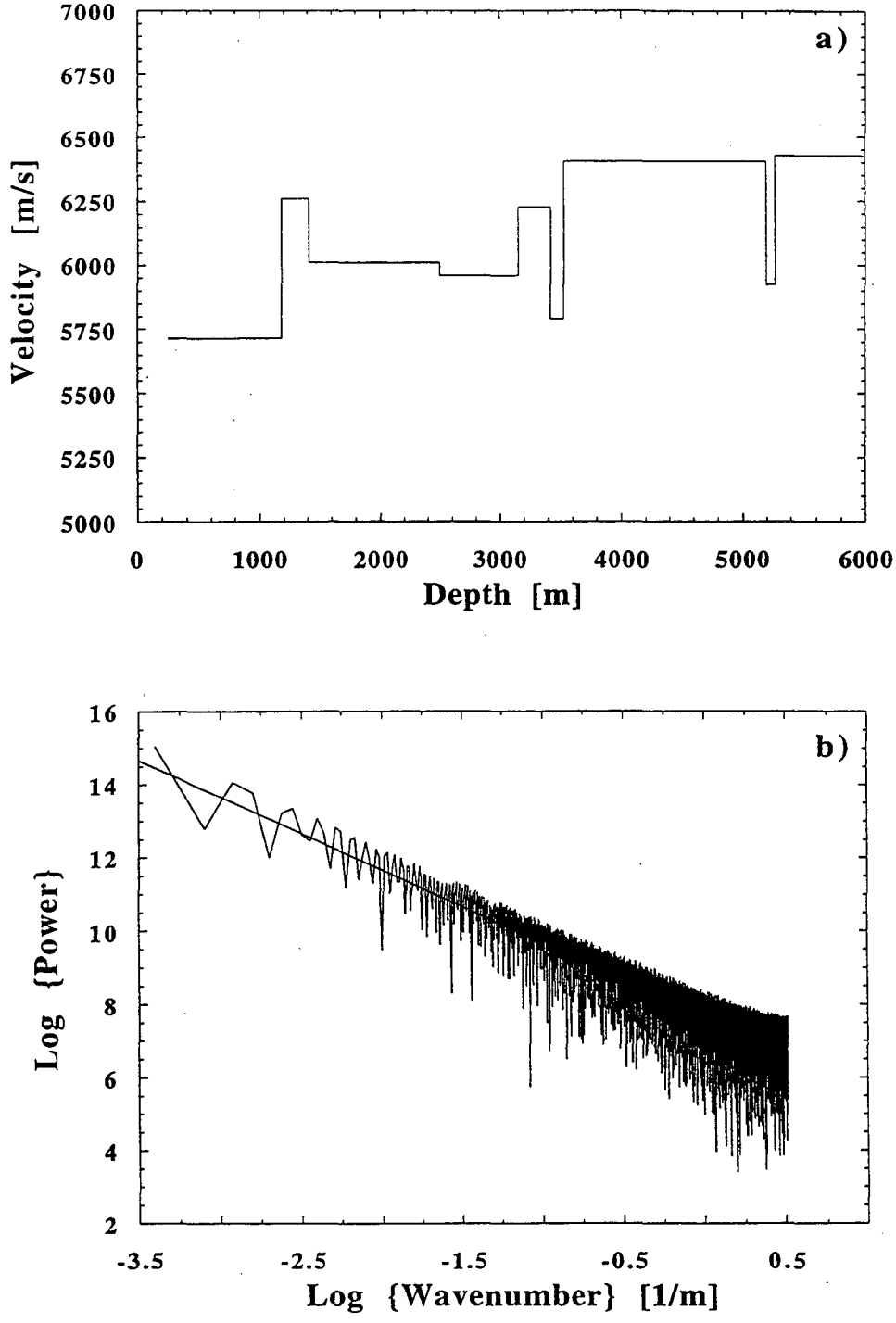

Figure 3

a) P wave velocity log averaged for each depth interval

b) Power spectrum of the averaged P wave velocity log and best least squares fit.

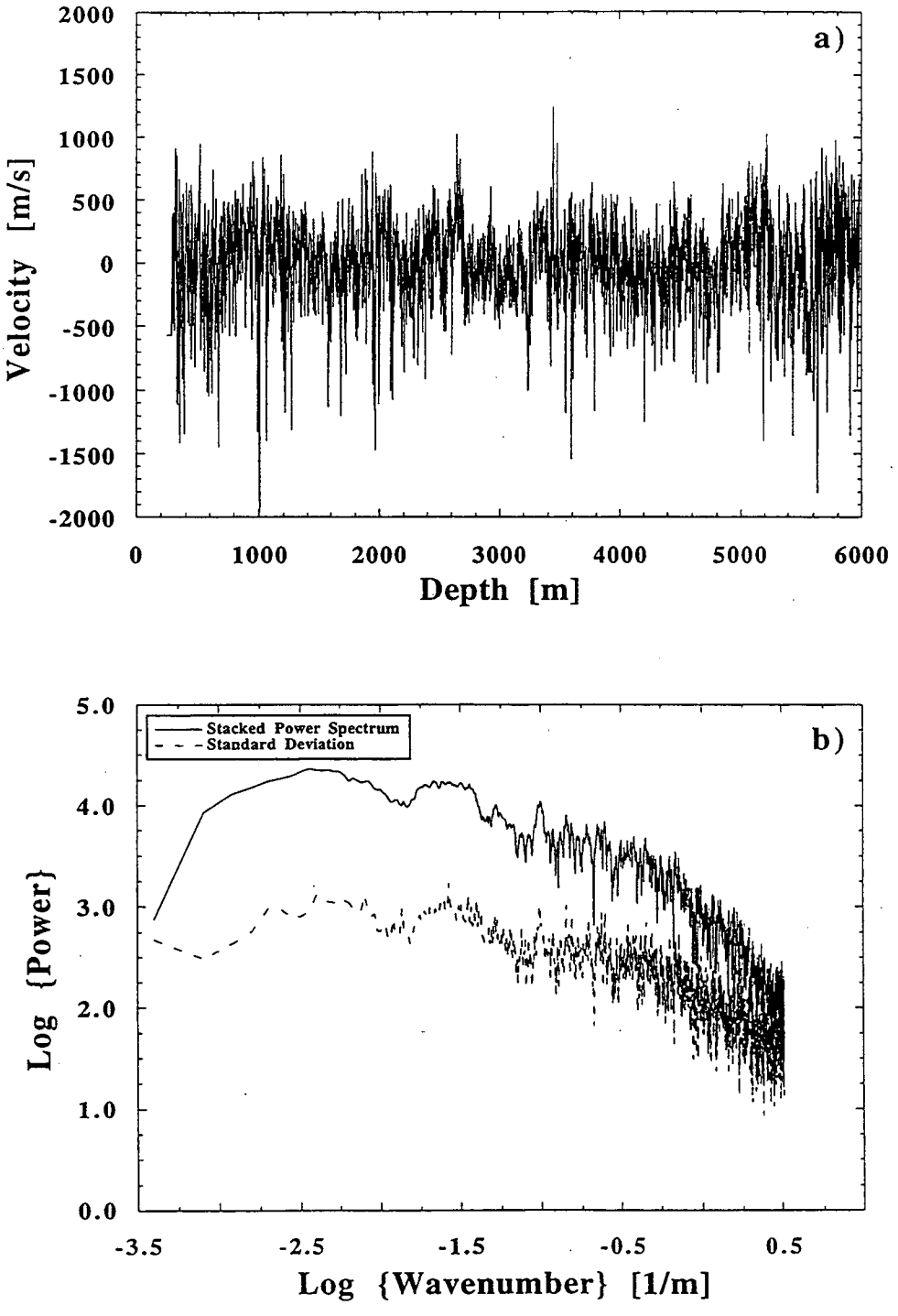

Figure 4

a) High frequency residual of the P wave velocity log,

b) Power spectrum (solid line) and standard deviation (dashed line) stacked over the nine depth intervals for the residual P wave velocity log.

structure, reveals constant properties over the whole depth range. Second, the power spectrum in Figure 4b resembles the Fourier transform of an exponential function: $P(f) = \frac{2a}{1 + k^2a^2}$, (Frankel and Clayton, 1986). Above we showed that the autocorrelation of the high frequency log data is best fit by an exponential function. Since the autocorrelation is a convolution of the signal with itself, a Fourier transform of the autocorrelation is equivalent to the power spectrum of the original signal. However, the Fourier transform of an exponential function, as given by Frankel and Clayton (1986), reveals a plateau for most of the spectrum, before it decays with a slope of -2. The difference in our spectrum is caused by intermediate scale lengths above 10 m that were not perfectly removed from the velocity log and can be seen as slight undulations in the detrended signal in Figure 4a. However, estimating the correlation length from the corner of the power spectrum yields an approximate value of a = 0.5 m which lies within the error limits of our correlation analysis. Thus the power spectrum analysis of the high frequency data independently confirms the results of the correlation analysis above. Further, these results suggest that the small scale structure as represented by the correlation length is most likely to be stationary at this site over the entire depth range of 6 km.

Modal Characteristics of the Medium

The modal character of a medium generally is addressed by investigating velocity histograms. However, even in media composed of two distinct materials e.g. in an alternating sequence of sedimentary layers, the result often is a narrow twin-peaked histogram where the distinction between the two modes is complicated by noisy data, particularly in the case when velocities of the two materials do not differ by a large magnitude. The determination of the modality, however, is essential for the correct representation of the medium for numerical modeling of elastic wave propagation when statistical approaches are applied to describe the medium properties (Levander and Holliger, 1992). A problem which may arise in the use of velocities is that effects present in the elastic moduli and density may be diminished by the tendency to cancel each other in the equations for the P wave and S wave velocities, $\sqrt{\frac{K + \frac{4}{3}\mu}{\rho}}$ and $\sqrt{\frac{\mu}{\rho}}$, respectively. In that case it may be more revealing to investigate the modal characteristics using the elastic moduli and the density rather than velocities, as long as density

measurements are available. Figure 5a shows a V_p vs. V_s plot of the velocity values for the upper 6 km at the KTB site. Although the velocities for the two main formations, gneiss and metabasite, differ by about 10 %, no clear distinction is visible in the data. The separation in the elastic moduli produced values plotted in Figures 5b - 5d. A slight separation can be seen in the K vs. μ plot, with metabasites revealing larger values, although the scatter in the data would make it difficult to make a distinction based on the elastic values alone. However, the differentiation becomes evident in the K vs. ρ and μ vs. ρ plots. A distinction between the two geological units is possible with the metabasites plotting at higher density values. Thus for the case of the KTB site the two units reveal a bimodal character apparent in the elastic moduli and density, whereas the velocities exhibit this information only weakly.

3. Localization of elastic waves in the upper crust

Stratigraphic filtering as introduced by O'Doherty and Anstey (1971) is based on the fact that during elastic wave propagation in horizontally layered media, multiple reflections within one layer interfere destructively with the direct pulse, attenuating parts of it within every layer. As a consequence, the direct wave exponentially decays in amplitude and gradually is deprived of its high frequency energy. Therefore, the direct pulse broadens constantly and the observed arrival is continuously shifted to later times in the seismogram. The longer the propagation distance in the medium, the lower are the frequencies which are affected. The localization distance is referred to as the distance within which the amplitude of the waves decays exponentially, and is defined as (White et al., 1990):

$$l^{-1} \approx -\frac{1}{L} \ln |T| = \alpha \ , \qquad (2)$$

where T is the transmission coefficient at distance L in the medium, and α is the scattering attenuation coefficient. Convergence for l is assumed to be rapid, once L is much larger than l. However, l is also a function of T, and therefore, convergence depends on the strength of the scattering in the medium. In the following, we show that for a layered medium with properties taken from the KTB logs convergence of l is given even for cases where l is on the same order as L.

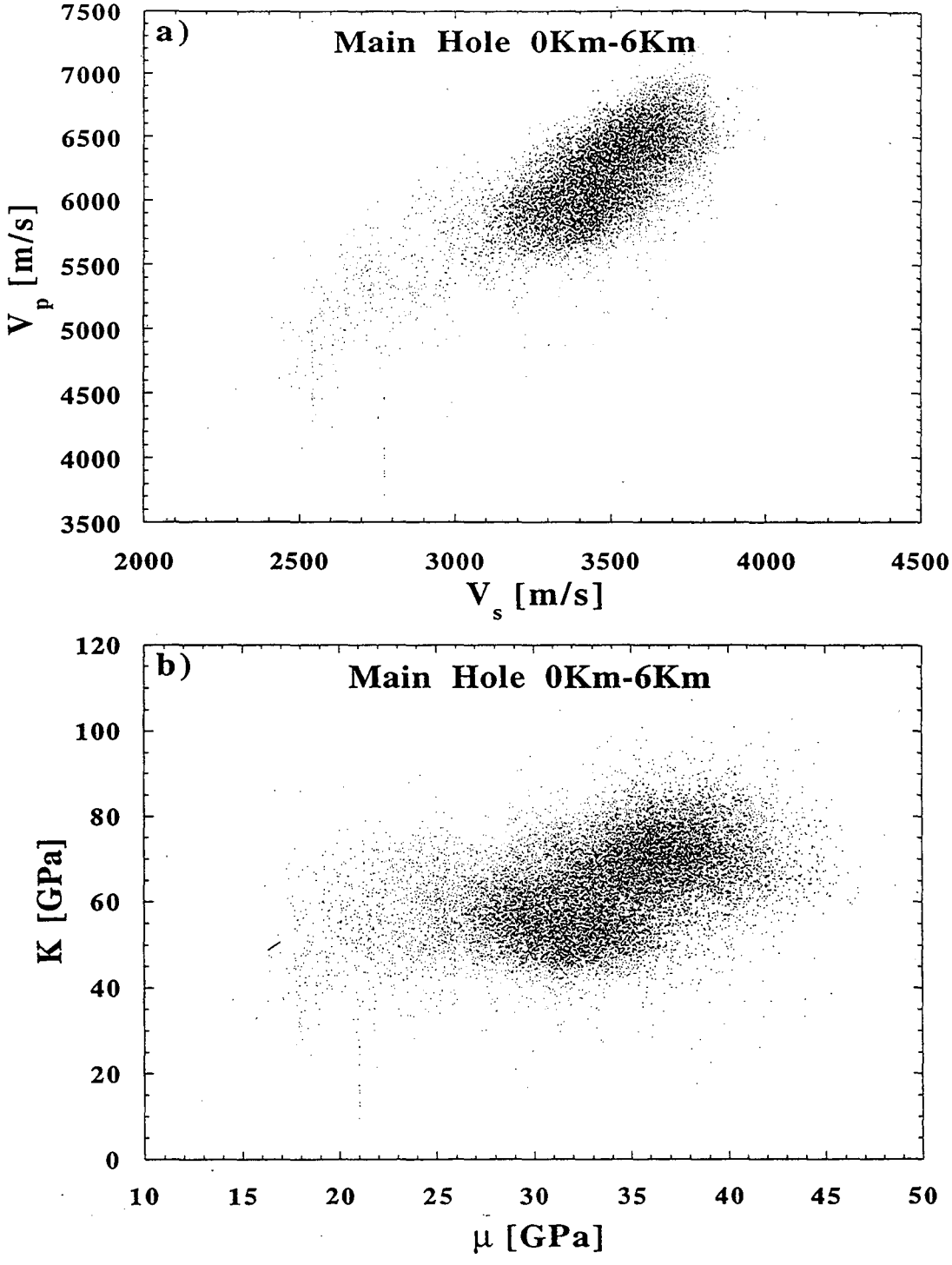

Figure 5 Scatter diagram of the elastic properties of the medium over a depth range of 6 km:

a) P wave velocity vs. S wave velocity,

b) Bulk modulus vs. shear modulus,

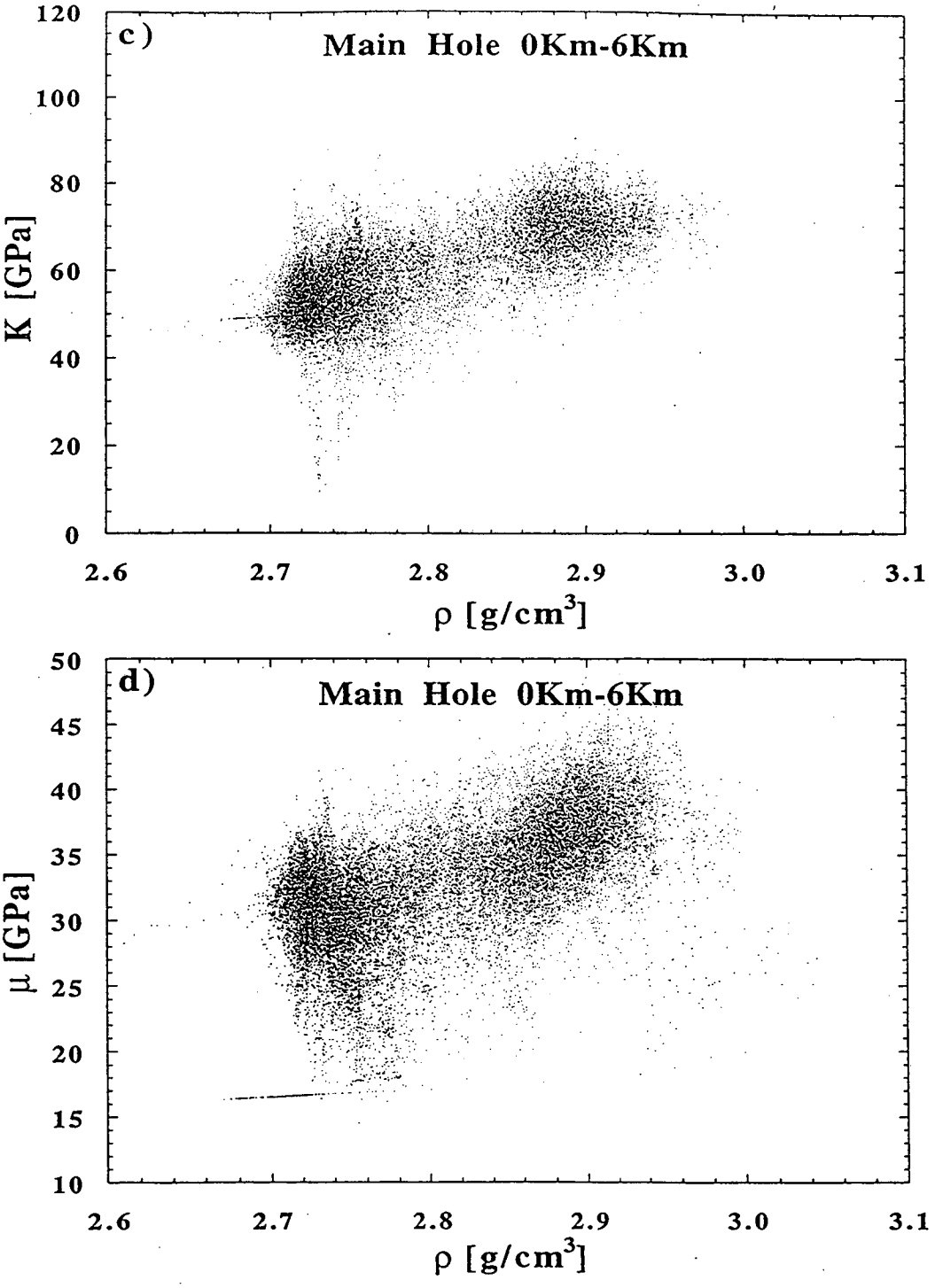

Figure 5 Scatter diagram of the elastic properties of the medium over a depth range of 6 km:

c) Bulk modulus vs. density,

d) Shear modulus vs. density.

We apply the propagator matrix approach (Kennett, 1985) to simulate one dimensional elastic wave propagation. Plane P, SV and SH waves are incident on a horizontally layered medium to study the localization effect on the three wavetypes. The angle of incident is 90^o to the layering to avoid conversion between the waves. In an initial set of calculations, the velocity and density logs from the main hole are used to simulate wave propagation over three distance ranges (2.85 km, 5.7 km, and 11.4 km) to study the effect of scattering. For the simulation with L = 5.7 km, we duplicate the density log to cover the upper 3 km of the crust, where no density information was available. However, in order to model the medium with L = 11.4 km, we duplicate the three logs in reverse order, thus simulating reflection of the wavefield at 5.7 km depth.

Figures 6a - 6c (P wave, SV wave, and SH wave, respectively) show the results for the propagation through a stack of layers (L = 11.4 km) using the natural log data. Because the angle of incidence is 90^o, there is no difference between the SV and the SH cases. We plot the reciprocal of the localization length as a function of frequency which ranges from 1 Hz to 10 kHz. Hence, the scattering process varies from Rayleigh in the low frequency range to Mie scattering in the intermediate range and ray theory scattering in the high frequency range. Rayleigh scattering is represented by a slope of 2 below 100 Hz, revealing a f^2 proportionality for one dimensional scattering. The change in slope indicates transition to the Mie scattering regime. Our interpretation suggests the onset of an interference pattern for the ray theoretical range. Hence, the first maximum between 1 kHz and 5 kHz (maximum attenuation) represents the strong scattering regime, when the wavelength is on the order of the correlation length in the medium, creating destructive interference of scattered waves. The next minimum for higher frequencies represents scattering of waves that produce constructive interference. Thereafter, we expect an alternating interference pattern with increasing frequencies. The average value of the pattern in this frequency range can be regarded as frequency independent; however, we caution the use of this interpretation, as it masks the physics governing the process and may cause misleading interpretations. The difference in shape between the curves for P and S wave in the high frequency range is caused by the longer wavelength of the P wave. Using the mean values of the P and S wave velocities of $\bar{V}_P = 6.1\ \frac{km}{s}$ and $\bar{V}_S = 3.4\ \frac{km}{s}$, the corresponding wavelengths for the first maximum amount to

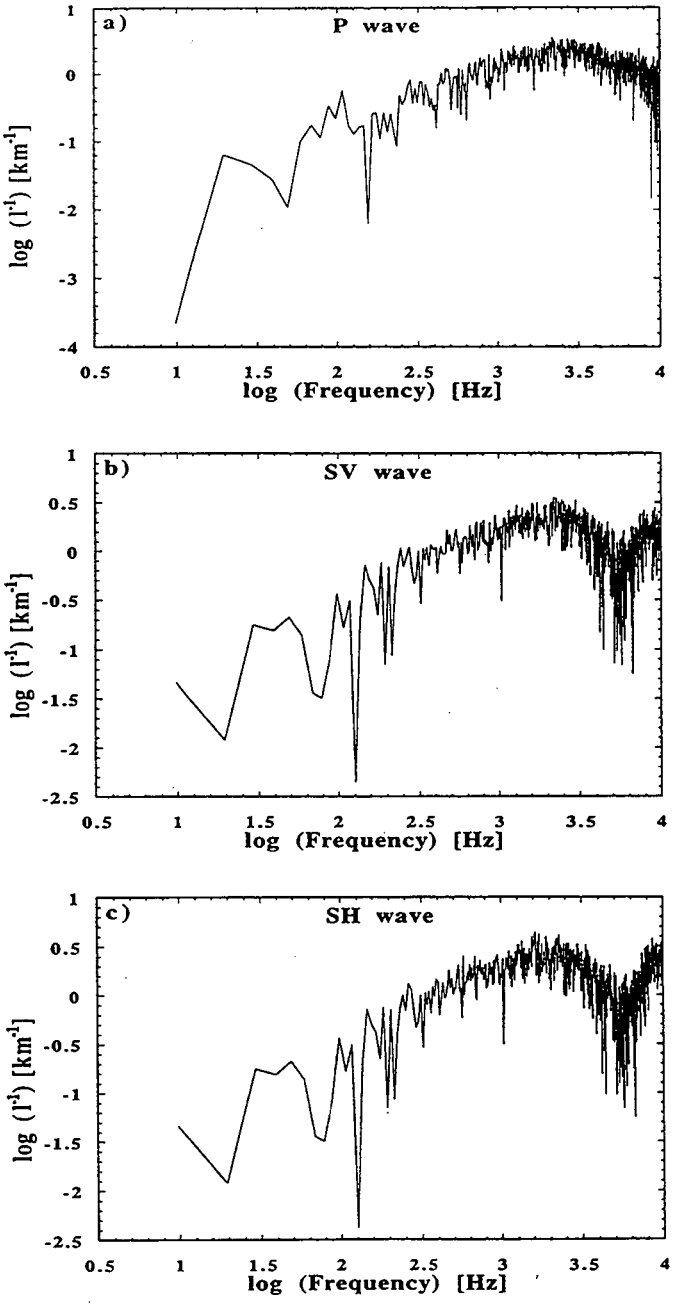

Figure 6 Localization plots computed for one dimensional elastic wave propagation using the real log data (L = 11.4 km):

a) localization of P waves,

b) localization of SV waves,

c) localization of SH waves.

λ_P = 2.4 m and λ_S = 2.0 m, respectively. Using the fact that the wavelength and correlation length of the medium coincide in the Mie scattering range, we see that the values match remarkably well with the correlation length deduced from the autocorrelation analysis of the well log data in the previous section.

It was stated for equation (2) (White et al., 1990) that localization occurs for $L \gg l$. However, this limit is an approximation and therefore the occurrence of localization has to be investigated for each case individually. The plots in Figure 6 indicate that all frequencies are affected by scattering attenuation. In order to determine whether the waves are exponentially attenuated (localized), we have to compare two curves for different propagation distances (different values of L), and investigate any possible change in l as a function of L and frequency. No change in l for certain frequencies for two different propagation lengths L indicates that the waves are already localized after propagation over the shorter distance, whereas a change in l shows that complete localization has not yet occurred. Note that localization, once established, is a frequency dependent function, and that the localization distance strongly depends on the standard deviation of the elastic parameters in the medium. Large standard deviations, causing stronger scattering, result in shorter localization lengths.

For a layered medium with properties equivalent to those at the KTB site, the localization plots for P and S waves do not change for frequency values above 30 Hz for propagation distances L $\geq$ 2.85 km. However, in order for localization to occur, the propagation length should be at least as large as the localization length. For a length of 2.85 km all frequencies above 200 Hz are localized, as the corresponding localization length is l = 2.5 km. Above this limit, the localization length decreases with increasing frequency. Since the corresponding localization length for f = 30 Hz is l ~ 10.0 km, transmission of energy in this frequency range is expected for the simulation with L = 2.85 km and L = 5.7 km. In the case of L = 11.4 km, however, the propagation distance is long enough for all frequencies above 30 Hz to be localized. This example shows that the mathematical limit $L \gg l$ does not necessarily have to be met for localization to occur in nature.

In a second set of calculations to verify the correlation functions of the medium estimated in section 2, we numerically create well logs and model elastic wave propagation through the medium, to

match the results obtained from the real log data. The numerical logs are created using normally distributed random values with the natural mean and standard deviation taken from the velocities and density. Three different filters, representing an exponential, a Gaussian, and a Von Karman correlation function, are applied to the data to model various media. For reasons of brevity, only the results of the SH wave for a propagation distance of L = 11.4 km are represented in Figure 7. Figure 7a shows the localization plot for a medium with an exponential correlation function modeling a characteristic length of a = 2.0 m. The graph shows a high degree of similarity with our previous results (Figure 6), revealing a slope of 2 for the Rayleigh scattering regime, followed by a gradual decrease in slope, and the interference pattern for frequencies in the ray theoretical regime. The result using the Gaussian correlation (a=2.0 m) is presented in Figure 7b. Up to the Mie scattering regime, the plot coincides with the results using the exponential function. Beyond 300 Hz, however, a steep descent and a very pronounced minimum over a broad frequency range indicates that a Gaussian correlation produces characteristic features that were not encountered in the real log data (Figure 6). Finally, the result modeling the Von Karman correlation function is given in Figure 7c. Previous investigations of the Von Karman function (not presented here) indicated a best fit for a characteristic length of a = 8.0 m. However, a break in slope from 2 to 1 above 300 Hz is notable and distinguishes these results from the previous model. Additionally, the interference pattern is not as well developed, thus rejecting the Von Karman function as a characteristic correlation function for the medium.

These simulations confirm the results of our correlation analysis, which indicates that the correlation of the small scale inhomogeneities is best modeled by an exponential function with a characteristic length of about 2 m.

Spectral Analysis of Localization Curves

The influence of the medium on wave propagation is evident in the interference pattern of the localization curves. This influence can be used to extract information about the properties of the medium. In the case of a sequence of horizontal layers, the medium can be regarded as a series of filters with specific reflection and transmission properties. For the case of elastic wave propagation in a medium with two alternating homogeneous layers of thickness h_1 and h_2 and corresponding velocities

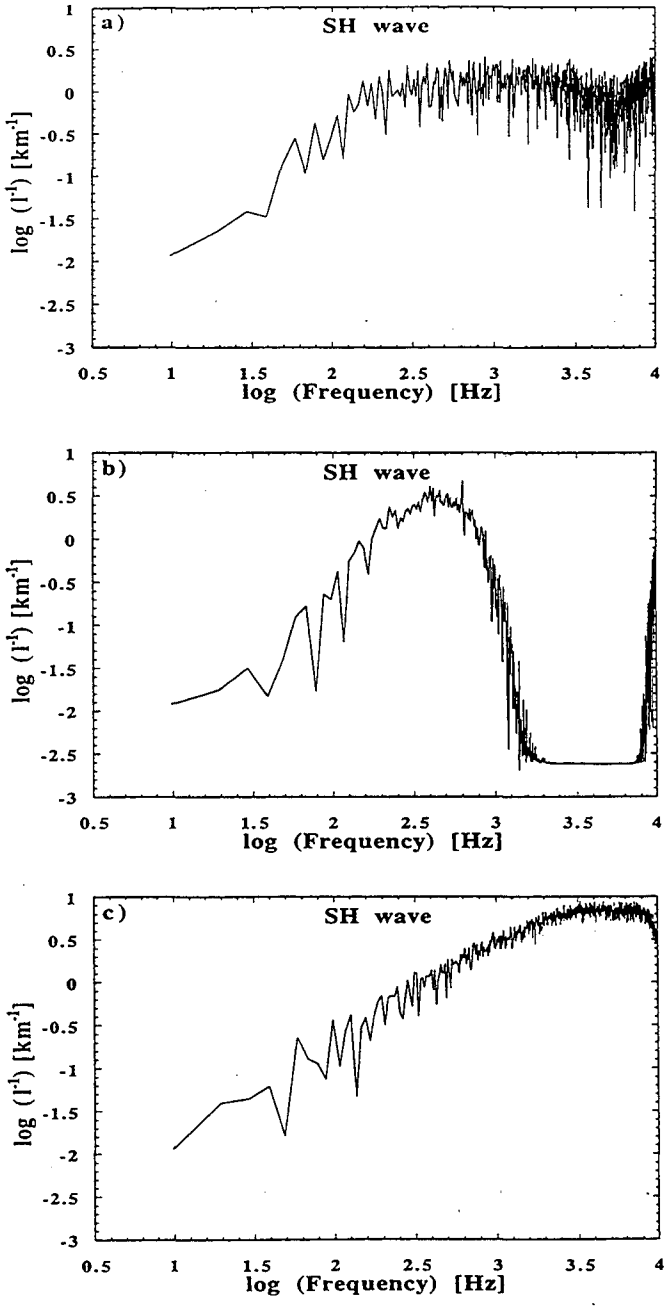

Figure 7 Localization plots for the SH wave computed for one dimensional elastic wave propagation based on simulated log data using various correlation functions (L = 11.4 km):

a) Exponential correlation function, a = 2.0 m,

b) Gaussian correlation function, a = 2.0 m,

c) Von Karman correlation function, a = 8.0 m.

V_1 and V_2, the spectrum of the localization curve as a function of $\frac{2h}{V}$ will reveal spectral peaks at the values $\frac{2h_1}{V_1}$ and $\frac{2h_2}{V_2}$. We successfully recovered these properties for a medium consisting of 100 layers each having a thickness of 1 km and alternating but constant velocities and densities in each layer. However, perturbing velocities and densities by adding a standard deviation of only 3% is sufficient to decrease the spectral peaks below noise level, thus removing all reliable information about the medium from the spectrum of the localization curve.

4. Conclusions

The correlation analysis of the high frequency velocity and density log data revealed a depth independent correlation length on the order of 2 m, with a standard deviation of 1.5 m. This indicates that, throughout the upper 6 km of the crust and within either of the two main geological units the material properties are correlated over distances less than about 2 m, but uncorrelated at greater distances. It also appeared that these statistical properties are stationary over the entire 6 km of the crust at the KTB site. Lateral variations were not observed. However, because of the close location of the main and pilot hole (180 m apart) this result carries little significance, as the two holes sample almost the same structure in relation to their depth extension. Therefore, the two main geological units consisting of gneiss and metabasalt which underwent metamorphic transformation appear to have a similar structure, and thus, seem to be indistinguishable with respect to velocity and density changes on the scale length of a few meters.

Different scale lengths in a medium are representative of different geological processes. Tectonic activities acting over scale lengths of several 100's of meters to several 10's of kilometers generate characteristic features that may differ from those created by petrogenic processes on smaller scales. The KTB V_p borehole logs support this idea. A model characterizing the broad velocity trend in the sequence of gneisses and metabasites revealed a power spectrum that could be fit by a slope of approximately -2, thus representing a fractal dimension over a scale length of ~ 3.5 km to ~ 100 m.

The small scale lengths were further investigated by analyzing the high frequency residual of the velocity log for which the broad trend was removed from the original data. Nine depth intervals over the whole log length (6 km) were stacked to independently confirm and evaluate the results of section one: stationarity of the small scale features throughout the upper crust and an exponential decay of the correlation function. A stable power spectrum with little variation and amplitudes larger than one standard deviation indicated stationarity of the high frequency signal. The shape of the power spectrum, resembling that of an exponential function, supports the result of the correlation analysis, as the Fourier transform of the autocorrelation function (a convolution of the signal with itself) is equivalent to the power spectrum of the original signal as determined above.

The analysis of the paper suggests that two different statistical processes are required to explain the KTB logs, a power law for the large scale lengths and an exponential law for the short scale lengths. As suggested by Wimmenauer et al. (1991), the gneisses are derived from graywackes indicating sedimentary deposition, whereas the metabasites are essentially derived from an intrusive complex (Schalwijk, 1991). Both sequences reveal a record of complex history in terms of deformation and metamorphosis which followed in time. The deformation is evident in the large scale signature of the log data revealing fractal character. The process of metamorphosis, however, altered the original rocks on a smaller scale, creating a homogeneous structure up to a size of about 2 meters. Within this range the rocks appear to be similar throughout the upper crust. Therefore we conclude that the deformation process differs from the metamorphosis through its characteristic scale lengths and the description by statistical analysis. However, this statistical analysis cannot determine which sequence was first deposited in time, nor, whether either deformation or metamorphosis preceded each other.

It should be pointed out that the description of the KTB log data obtained in this study is not unique. Wu et al. (1994), working only with the velocity logs, chose to separate the logs into a deterministic and a random component, where the deterministic part was taken to be a linear function of depth. The power spectrum of the random component was found to have a power law form with a slope of about -1.1. The presence of a different behavior at dimensions less than 10 m was noted, but not analyzed.

Statistical approaches are common tools for the treatment of elastic wave propagation in complicated heterogeneous media. However, this approach requires knowledge about the statistical properties of the medium, such as mean values and standard deviations, distribution of elastic properties, and modal character of the distribution. In the case of elastic wave propagation the most studied parameters are the P and S-wave velocities of the medium. The geology at the KTB site clearly exhibits a bimodal character established by the sequence of gneisses and metabasites as seen in the gamma ray log. However, investigating scatter plots of V_p vs. V_s this property was only poorly resolved although the velocity difference between the two sequences is about 10%. In contrast, the subdivision in the elastic moduli revealed that scatter plots of bulk or shear modulus versus density clearly exhibit the bimodal character, as the metabasites plot at higher density values, thus separating the two geologic units and revealing the true underlying character of the medium. Therefore, whenever density measurements are available, an investigation of the fundamental elastic properties is recommended.

The effect of inhomogeneities on the propagation of elastic waves, and the possibility of total wave attenuation by scattering processes only, as suggested by O'Doherty and Anstey (1971), was investigated for the upper crust at the KTB site. Our results indicate that all frequencies are affected by scattering processes. The trend of the localization length as a function of frequency allows characteristic parameters of the medium to be determined. From the scattering regime, where the wavelength is on the order of the correlation length, we determined the wavelength as λ_P = 2.4 m and λ_S = 2.0 m, supporting the results of the correlation analysis. Therefore, this method proves to be a fast way to estimate the dominant correlation length in the medium. Comparison of several localization plots for different propagation distances revealed that total attenuation due to elastic scattering is evident for distances longer than 2.5 km for frequencies above 200 Hz. When the propagation distance increases to 10 km, however, localization occurs for all waves with frequencies as low as 30 Hz. These results can have an impact on seismic surveys, as it suggests that there is a practical limit on the distance to which high frequencies can be propagated in a coherent fashion.

It should be pointed out that certain assumptions, like a one-dimensional layered medium, were made in the simulations of wave propagation which might not be appropriate for an actual experiment

at the KTB site. Additionally, anelastic attenuation which has not been taken into account in our wave propagation will lead to additional losses in transmitted energy, and therefore, the limit of wave propagation will further decrease.

The simulation of real log data, testing a Gaussian, Von Karman, and exponential distribution, was intended to confirm the results of the correlation analysis, and to repeat the wave propagation for real log data. By comparing the localization plots, we were able to dismiss a Gaussian or Von Karman function as a representation for the correlation of the velocity and density in the medium. The results showed good agreement for an exponential distribution with correlation length a=2.0 m, and independently confirmed the values of our correlation analysis.

5. Acknowledgements

The authors are grateful to Julie Najita and Valeri Korneev for their helpful discussions. Data were gathered under grant RG 9001-0 of the German Federal Ministry of Research and Technology. We would like to thank the KTB Project Management Group, Hannover, for release and permission to use the KTB well log data. Data processing was done at the Center for Computational Seismology, Lawrence Berkeley Laboratory, under support from the Director, Office of Energy Research, Office of Basic Energy Sciences, Geosciences Program, through U.S. Department of Energy contract DE-AC03-76SF00098.

6. References

Banik, N.C., Lerche, I., and Shuey, R.T., 1985a, Stratigraphic filtering, Part I: Derivation of the O'Doherty-Anstey formula, *Geophysics*, **50**, 2768-2774.

Banik, N.C., Lerche, I., and Shuey, R.T., 1985b, Stratigraphic filtering, Part II: Model spectra, *Geophysics*, **50**, 2775-2783.

Frankel, A. and Clayton, R.W., 1986, Finite difference simulations of seismic scattering: implications for the propagation of short-period seismic waves in the crust and models of heterogeneity, *J. Geophys. Res.*, **91**, 6465-6489.

Kennett, B.L.N., 1985, Seismic Waves Propagation in Stratified Media, *Cambridge University Press.*

Levander, A.R. and Holliger, K., 1992, Small-scale heterogeneity and large-scale velocity structure of the continental crust, *J. Geophys. Res.*, **97,** 8797-8804

Lich, S., Dyster, J., Godizart, G., Keyssner, S., and de Wall, H., 1992, German Continental Deep Drilling Program (KTB) - geological survey of the Hauptbohrung 0 - 6000 m, *in KTB Report 92-2, Emmermann, R., Dietrich, H.-G., Lauterjung, J., and Woehrl, Th., eds.*, Niedersaechsisches Landesamt fuer Bodenforschung.

Marple, S.L. and Englewood, C.N.J., 1987, Digital Data Analysis, *Prentice-Hall.*

O'Doherty, R.F. and Anstey, N.A., 1971, Reflections on Amplitudes, *Geophysical Prospecting,* **19,** 430-458.

Shapiro, S.A. and Zien, H., 1993, The O'Doherty-Anstey formula and localization of seismic waves, *Geophysics,* **58,** 736-740.

Sheng, P., Ed., 1990, Scattering and localization of classical waves in random media, *World Scientific Publ. Co., Inc.*

White, B., Sheng P. and Nair B., 1990, Localization and backscattering spectrum of seismic waves in stratified lithology, *Geophysics,* **55,** 1158-1165.

Wu, R.S. and Aki, K., 1985, Elastic wave scattering by a random medium and the small-scale inhomogeneities in the lithosphere, *J. Geophys. Res.*, **90,** 10261-10273.

Wu, R.S., Xu, Z. and Li X.P., 1994, Heterogeneity spectrum and scale-anisotropy in the upper crust revealed by the German Continental Deep-Drilling (KTB) Holes, *Geophys. Res. Lett.*, **21,** 911-914.

LAWRENCE BERKELEY LABORATORY
UNIVERSITY OF CALIFORNIA
TECHNICAL AND ELECTRONIC
INFORMATION DEPARTMENT
BERKELEY, CALIFORNIA 94720